The Calcium Channel Blockers, 1,4-Dihydropyridines, Are Substrates of the Multidrug Resistance-Linked ABC Drug Transporter, ABCG2†

Suneet Shukla,‡ Robert W. Robey,§ Susan E. Bates,§ and Suresh V. Ambudkar*,‡

Laboratory of Cell Biology and Cancer Therapeutics Branch, Center for Cancer Research, National Cancer Institute, National Institutes of Health, Bethesda, Maryland 20892

Received March 20, 2006; Revised Manuscript Received May 9, 2006

ABSTRACT: The human ATP-binding cassette transporter, ABCG2, confers resistance to multiple chemotherapeutic agents and also affects the bioavailability of different drugs. [^{125}I]Iodoarylazidoprazosin (IAAP) and [^{3}H]azidopine were used for photoaffinity labeling of ABCG2 in this study. We show here for the first time that both of these photoaffinity analogues are transport substrates for ABCG2 and that [^{3}H]azidopine can also be used to photolabel both wild-type R482-ABCG2 and mutant T482-ABCG2. We further used these assays to screen for potential substrates or modulators of ABCG2 and observed that 1,4-dihydropyridines such as nicardipine and nifedipine, which are clinically used as antihypertensive agents, inhibited the photolabeling of ABCG2 with [^{125}I]IAAP and [^{3}H]azidopine as well as the transport of these photoaffinity analogues by ABCG2. Furthermore, [^{3}H]nitrendipine and bodipy-Fl-dihydropyridine accumulation assays showed that these compounds are transported by ABCG2. These dihydropyridines also inhibited the efflux of the known ABCG2 substrates, mitoxantrone and pheophorbide-a, from ABCG2-overexpressing cells, and nicardipine was more potent in inhibiting this transport. Both nicardipine and nifedipine stimulated the ATPase activity of ABCG2, and the nifedipine-stimulated activity was inhibited by fumitremorgin C, suggesting that these agents might interact at the same site on the transporter. In addition, nontoxic concentrations of dihydropyridines increased the sensitivity of ABCG2-expressing cells to mitoxantrone by 3−5-fold. In aggregate, results from the photoaffinity labeling and efflux assays using [^{125}I]IAAP and [^{3}H]azidopine demonstrate that 1,4-dihydropyridines are substrates of ABCG2 and that these photolabels can be used to screen new substrates and/or inhibitors of this transporter.

The overexpression of ATP-binding cassette (ABC)[1] transporters such as P-glycoprotein (P-gp, ABCB1) and multidrug resistance protein 1 (MRP1, ABCC1) has been shown to confer resistance to a variety of chemotherapeutic agents by effluxing drug substrates from cells in an energy-dependent manner. ABCG2 [also called mitoxantrone resistance-associated protein (MXR), breast cancer resistance protein (BCRP), or placenta specific ABC transporter (ABCP)], a half-transporter, was first found in multidrug resistant tumor cells that did not express either P-gp or MRP1 (*1*−*3*). It is a 655-amino acid integral membrane protein of the ABCG subfamily of ABC transporters, whose overexpression plays a major role in the multidrug resistance phenotype of malignant cells by actively effluxing cytotoxic compounds such as doxorubicin, mitoxantrone, camptothecins including topotecan, and SN-38 (*3*−*5*). Overexpression of ABCG2 has also been observed in mitoxantrone- and topotecan-selected breast, colon, ovarian, and gastric carcinoma cell lines and in choriocarcinoma cell lines, leading to the drug resistant phenotype of these cell lines (*6*, *7*).

It has been shown that spontaneous mutations occur in drug-selected cells at amino acid position 482 of this transporter. While the wild-type transporter has arginine, the mutant has a glycine or threonine at this position (*8*, *9*). There are several reports demonstrating that substitutions at position 482 induce major alterations in both the transport activity and substrate specificity of the transporter (*9*−*12*). Recent reports have attributed the secretion of several xenotoxins, dietary carcinogens, and antibiotics such as nitrofurantoin into breast milk to highly induced levels of Abcg2 in the luminal membrane of alveoli of the mammary gland during lactation in mice (*13*, *14*). In addition, the drug-induced upregulation of ABCG2 was also thought to reduce the oral bioavailability of imatinib or irinotecan (*15*, *16*), thereby altering the pharmacokinetics of this drug. Therefore, studies involving the determination of drug interactions with ABCG2 would provide important information regarding the oral bioavailability and the systemic toxicity of ABCG2 substrates and inhibitors.

In this study, we have used photoaffinity labeling and accumulation assays to screen potential substrates or modulators of ABCG2 and have shown that the photoaffinity analogues [^{125}I]iodoarylazidoprazosin (IAAP) and [^{3}H]azi-

† This work was supported by the Intramural Research Program of the National Institutes of Health, National Cancer Institute, Center for Cancer Research.

* To whom correspondence should be addressed. Phone: (301) 402-4178. Fax: (301) 435-8188. E-mail: ambudkar@helix.nih.gov.

‡ Laboratory of Cell Biology.

§ Cancer Therapeutics Branch.

[1] Abbreviations: ABC, ATP-binding cassette; ABCP, placenta specific ABC transporter; BCRP, breast cancer resistance protein; BeFx, beryllium fluoride; DMSO, dimethyl sulfoxide; FBS, fetal bovine serum; FTC, fumitremorgin C; HEK, human embryonic kidney; MXR, mitoxantrone resistance-associated protein; MDR, multidrug resistance; PAGE, polyacrylamide gel electrophoresis; P-gp, P-glycoprotein.

10.1021/bi060552f
Published on Web 07/01/2006

dopine can be used to photolabel both R482-ABCG2 (wild type) and T482-ABCG2 (mutant). Accumulation assays with these compounds demonstrated that these photoaffinity agents are actually transported by ABCG2. Thus, because of their use in photoaffinity labeling to assess binding as well as transport, these agents should prove to be useful in screening new substrates and inhibitors of this transporter. We show here using these photolabels and other biochemical assays that the two dihydropyridines, nicardipine and nifedipine, which are used as antihypertensive drugs in the clinic, interact with both wild-type and mutant ABCG2 and are also transported by this transporter.

MATERIALS AND METHODS

Chemicals. RPMI media, penicillin, streptomycin, trypsin-EDTA, Dulbecco's phosphate-buffered saline (PBS), and Iscove's modified Dulbecco's medium (IMDM) were purchased from Gibco (Carlsbad, CA). Minimum Essential Medium, Eagle (MEM) was purchased from ATCC (Manassas, VA). G418 was procured from RPI Corp. (Mt. Prospect, IL). Mitoxantrone, MTT [3-(4,5-dimethylthiazol-2-yl)-2,5-diphenyltetrazolium bromide] dye, ouabain, and all other chemicals were purchased from Sigma (St. Louis, MO). The radiolabeled [^{125}I]IAAP (2200 Ci/mmol) and [^{3}H]-nitrendipine (87 Ci/mmol) were purchased from PerkinElmer Life Sciences (Wellesley, MA). [α-^{32}P]-8-Azido-ATP (15−20 Ci/mmol) and [^{3}H]azidopine (60 Ci/mmol) were procured from Affinity Labeling Technologies (Lexington, KY) and Amersham Biosciences (Piscataway, NJ), respectively. The BXP-21 monoclonal antibody was obtained from Kamiya Biomedical Co. (Seattle, WA). Bodipy-Fl-dihydropyridine was purchased from Invitrogen (Carlsbad, CA).

Cell Lines and Culture Conditions. HEK-293 cells were stably transfected with either an empty pcDNA3.1 vector (pcDNA3.1-HEK) or pcDNA3.1 containing ABCG2 encoding either an arginine (R482-HEK) or a glycine (G482-HEK) at position 482. The stable transfectants of HEK-293 cells were maintained in MEM supplemented with 10% FCS, penicillin, streptomycin, and 2 mg/mL G418 (*8*). MCF-7 cells and sublines were cultured in RPMI with 10% FBS. MCF-7 FLV1000 (R482-ABCG2) cells were maintained in 1 μg/mL flavopiridol, and MCF-7 AdVp3000 (T482-ABCG2) cells were maintained in 3 μg/mL doxorubicin and 5 μg/mL verapamil (*10*, *17*).

Fluorescent Drug Accumulation Assay. The accumulation assays were performed as described previously with minor modifications (*10*). Briefly, the cells were trypsinized and resuspended in phenol red-free IMDM with 5% FBS. Mitoxantrone (5 μM), pheophorbide-a (5 μM), or bodipy-Fl-dihydropyridine (0.5 μM) was added to 5×10^5 cells in 4 mL of IMDM in the presence or absence of 10 μM ABCG2 inhibitor, fumitremorgin C (FTC), or in various concentrations of dihydropyridines and incubated at 37 °C for 45 min. The cells were then pelleted, resuspended in PBS containing 0.1% BSA, and analyzed immediately with a FACSort flow cytometer (Becton-Dickinson Immunocytometry Systems, San Jose, CA). For all samples, 10 000 events were counted and analysis was performed with CellQuest (Becton-Dickinson Immunocytometry Systems). The mean fluorescence intensity was calculated using statistics in CellQuest.

Isolation of Crude Membranes from ABCG2-Expressing HEK or MCF-7 Cells. Membranes from control MCF-7, MCF-7 FLV1000, or MCF-7 AdVp3000 cells were prepared as described elsewhere (*18*). The protein content was estimated using an amido black B dye binding assay, as described previously (*18*).

Photo-Cross-Linking of ABCG2 with [^{125}I]IAAP and [^{3}H]-Azidopine. Crude membranes (1 mg of protein/mL) from the MCF-7 FLV1000 or MCF-7 AdVp3000 cells were incubated with various concentrations of dihydropyridines or 20 μM FTC for 10 min at room temperature in 50 mM Tris-HCl (pH 7.5); 3−6 nM [^{125}I]IAAP (2200 Ci/mmol) or 0.5 μM [^{3}H]azidopine (60 Ci/mmol) was added, and the samples were incubated for an additional 5 min under subdued light. The samples were then illuminated with a UV lamp assembly (PGC Scientifics, Gaithersburg, MD) fitted with two black light (self-filtering) UV-A long-wave F15T8BLB tubes (365 nm, 15 W) for 10 min at room temperature (21−23 °C). The labeled ABCG2 was immunoprecipitated via addition of 800 μL of RIPA buffer containing 1% aprotinin followed by addition of 10 μg of BXP-21 antibody. The samples were incubated at 4 °C for 3 h, and 100 μL of 20% (w/v) protein A−Sepharose beads (Amersham Biosciences) was added with further incubation at 4 °C for 16 h. The protein A−Sepharose beads were pelleted by centrifugation of the samples at 13 000 rpm for 5 min at 4 °C and washed with RIPA containing 1% aprotinin. Next 25 μL of 2× SDS−PAGE sample buffer was added, and the samples were incubated at 37 °C for 1 h. This was followed by the addition of 25 μL of water and further incubation at 37 °C for 30 min. The samples were separated on a 7% Tris-acetate gel at a constant voltage. The [^{3}H]azidopine gel was incubated with Fluoro-Hance (RPI Corp.) for 30−45 min. Both gels were dried and exposed to Bio-Max MR film (Eastman Kodak, Rochester, NY) for 3−6 days at −80 °C. The incorporation of [^{125}I]IAAP or [^{3}H]azidopine (from the autoradiogram) into the ABCG2 band was quantified by estimating the radioactivity of this band using the STORM 860 phosphorimager (Molecular Dynamics, Sunnyvale, CA) and ImageQuaNT, as described previously (*18*).

[^{125}I]IAAP, [^{3}H]Azidopine, and [^{3}H]Nitrendipine Accumulation Assay. MCF-7, MCF-7 FLV1000, or MCF-7 AdVp3000 cells (2.5×10^5 cells/well) were grown in a monolayer in a 24-well tissue culture plate at 37 °C in the presence of 5% CO_2 in RPMI supplemented with 10% FBS. The assay was initiated by incubating cells with 1.5 nM [^{125}I]-IAAP, 25 nM [^{3}H]azidopine, or 25 nM [^{3}H]nitrendipine in the absence or presence of 10 μM FTC or 50 μM nicardipine at 32 °C for 0−60 min in 0.3 mL of RPMI supplemented with 10% FBS under subdued light (to avoid photo-cross-linking). After being incubated, cells were washed with PBS and lysed by incubation with 0.3 mL of trypsin-EDTA/well at 37 °C for 30 min. The cell lysates were transferred to scintillation vials containing 5 mL of Bio-Safe II scintillation fluid, and the radioactivity was measured in a scintillation counter. Cells washed with PBS immediately after addition of the assay mix were used as the zero minute time point. The value for accumulated [^{125}I]IAAP, [^{3}H]azidopine, or [^{3}H]-nitrendipine at time zero (within 3−5 s) was subtracted from a given time point as the level of nonspecific binding of these compounds to the cells. The accumulation of labeled compounds was expressed as picomoles per 1 million cells.

These assays were carried out at 32 °C to slow the rate of efflux from these cells in an effort to study the accumulation and efflux in a time-dependent manner.

ATPase Assay. Crude membranes from HEK-ABCG2 cells were analyzed for both basal and drug-stimulated ATP hydrolysis by colorimetric detection of inorganic phosphate release, as described previously (*19*). Crude membranes of R482-HEK-293 and pcDNA3.1-HEK-293 cells (100 μg of protein/mL) were incubated at 37 °C with varying concentrations of dihydropyridines, prazosin, or FTC in the presence and absence of beryllium fluoride (BeFx, 0.2 mM beryllium sulfate and 2.5 mM sodium fluoride) in ATPase assay buffer [0.05 mM KCl, 5 mM sodium azide, 2 mM EGTA, 10 mM $MgCl_2$, 1 mM DTT, and 50 mM MOPS (pH 7.5)] for 5 min. The reaction was started by the addition of 5 mM ATP and was stopped by the addition of 0.1 mL of a 5% SDS solution. The amount of inorganic phosphate released and the BeFx-sensitive ATPase activity of ABCG2 were determined as described previously (*19*).

Binding of [α-^{32}P]-8-Azido-ATP to ABCG2. Crude membranes from MCF-7 AdVp3000 cells were incubated with 25 μM dihydropyridines or 5 mM ATP for 10 min at 4 °C in ATPase assay buffer (without DTT). [α-^{32}P]-8-Azido-ATP (10 μM, 10 μCi/nmol) was added under subdued light and the mixture incubated for an additional 5 min at 4 °C. The samples were then illuminated with a UV lamp (365 nm) for 10 min and were separated on a SDS−7% Tris-acetate polyacrylamide gel at a constant voltage. The gel was dried under vacuum, exposed to X-ray film for 1−3 days at −70 °C.

Cytotoxicity Assays. The cytotoxicity of dihydropyridines in control and ABCG2-expressing cells was determined by the MTT assay as described previously (*18*). Briefly, cells (5×10^3) were plated overnight into a 96-well microtiter plate in triplicate. Various concentrations of dihydropyridines or drugs were added to the medium, and the plates were incubated for an additional 72 h. The medium was aspirated; 100 μL of MTT dye was added to each well, and the samples were incubated for a further 3−4 h. The MTT solution was aspirated, and the formazan product was dissolved in 200 μL of 2-propanol. The absorbance in each well was measured at 570 nm with a reference wavelength of 650 nm. The concentration of dihydropyridines which produced 50% inhibition of growth (IC_{50}) was calculated from linear regression analysis of the linear portion of the growth curves. The fractional absorbance was calculated with the formula % cell survival = (mean absorbance in the test well)/(mean absorbance in control wells) × 100, as previously described (*18*).

RESULTS

Dihydropyridines Inhibit the Photolabeling of ABCG2 with [^{125}I]IAAP and [^{3}H]Azidopine. [^{125}I]IAAP and [^{3}H]azidopine, the photoaffinity analogues of prazosin and dihydropyridine, respectively, have been used to characterize the drug binding sites of P-gp and other ABC transporters (*20*−*23*). We used these analogues to photolabel both wild-type (R482) and mutant (T482) ABCG2 (Figure 1) and further studied the interactions of potential substrates and inhibitors with ABCG2 using these labels. In our preliminary screening studies, we observed that 1,4-dihydropyridines inhibited the photolabeling of both wild-type and mutant ABCG2 with these two analogues. As shown in Figure 1, the crude membranes (20 μg) from MCF-7 FLV1000 (R482-ABCG2) or MCF-7 AdVp3000 (T482-ABCG2) cells were incubated with 20 μM nicardipine, nifedipine, or FTC at room temperature for 10 min and photolabeled with either 3−6 nM [^{125}I]IAAP (2200 Ci/mmol) (Figure 1a,b) or 0.5 μM [^{3}H]-azidopine (Figure 1c,d) as described in Materials and Methods. [^{125}I]IAAP was able to photolabel wild-type and mutant ABCG2 from MCF-7 FLV1000 (Figure 1a, lane 1) and MCF-7 AdVp3000 (Figure 1b, lane 1) cells, respectively, which was consistent with a previous report (*24*). This labeling was inhibited by both nicardipine and nifedipine (Figure 1a,b, lanes 3 and 4). The inhibition of incorporation of [^{125}I]IAAP into ABCG2 by nicardipine was comparable to, or more than, that by FTC (Figure 1a−d, lane 2), which is a specific inhibitor of this transporter (*25*−*28*). [^{3}H]-Azidopine, which itself is a dihydropyridine analogue, was also able to photolabel both the wild type (Figure 1c, lane 1) and the mutant ABCG2 (Figure 1d, lane 1). This photolabeling was also inhibited by the presence of 20 μM nicardipine and nifedipine (Figure 1c,d, lanes 3 and 4). Nicardipine appeared to be more effective in inhibiting the photolabeling of both wild-type and mutant ABCG2 with [^{125}I]IAAP and [^{3}H]azidopine. This inhibition of [^{125}I]IAAP (Figure 2a,b) or [^{3}H]azidopine (Figure 2c,d) labeling by nicardipine of both wild-type (Figure 2a,c) or mutant ABCG2

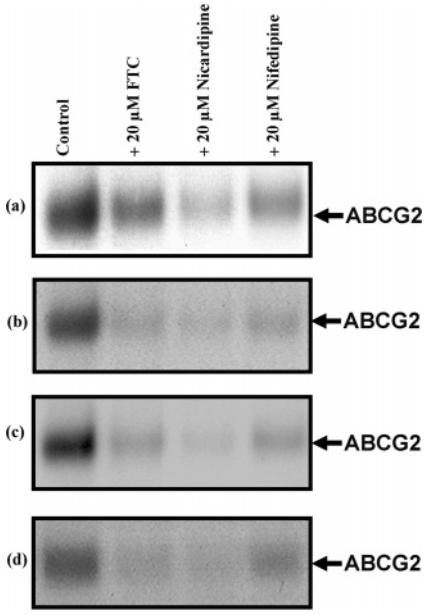

FIGURE 1: Dihydropyridines inhibit the photolabeling of wild-type and mutant ABCG2 with [^{125}I]IAAP and [^{3}H]azidopine. Crude membranes (500 μg/mL) from MCF-7 FLV1000 (a and c) and MCF-7 AdVp3000 (b and d) cells were incubated with the indicated drug (20 μM) for 10 min at room temperature in 50 mM Tris-HCl (pH 7.5), and 3−6 nM [^{125}I]IAAP (2200 Ci/mmol) (a and b) or 0.5 μM [^{3}H]azidopine (60 Ci/mmol) (c and d) was added and the mixture incubated for an additional 5 min under subdued light. The samples were then cross-linked with a UV lamp (365 nm) for 10 min at room temperature and were processed after immunoprecipitation with the BXP-21 antibody, as described in Materials and Methods. The autoradiograms from a representative experiment are shown, and the arrow represents the position of ABCG2. A representative experiment from three independent experiments is shown here.

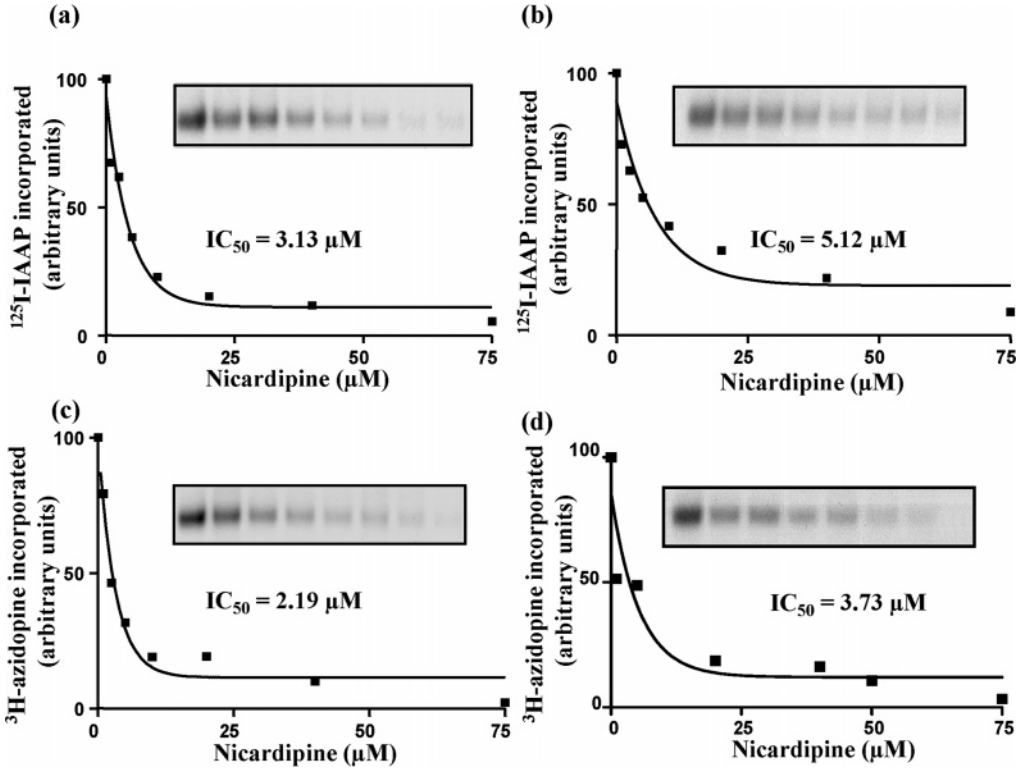

FIGURE 2: Nicardipine inhibits, in a concentration-dependent manner, the photolabeling of the wild-type and mutant ABCG2 with [^{125}I]-IAAP and [^{3}H]azidopine. The crude membranes (500 μg/mL) from MCF-7 FLV1000 (a and c) and MCF-7 AdVp3000 (b and d) cells were incubated with increasing concentrations (0−75 μM) of nicardipine for 10 min at room temperature in 50 mM Tris-HCl (pH 7.5), and 3−6 nM [^{125}I]IAAP (2200 Ci/mmol) (a and b) or 0.5 μM [^{3}H]azidopine (60 Ci/mmol) (c and d**)** was added. The samples were processed as described in the legend of Figure 1. The radioactivity incorporated into the ABCG2 band (autoradiogram in the inset) was quantified as described in Materials and Methods, and the data were fit using Graphpad Prism version 2.0. A representative experiment from three independent experiments is shown here. There was <10% variation in each data set. The IC$_{50}$ values were calculated as the concentration of nicardipine which inhibited the incorporation of [^{125}I]IAAP or [^{3}H]azidopine to 50% of the control values (in the absence of any dihydropyridine).

(Figure 2b,d) was concentration-dependent, with IC$_{50}$ values ranging from 2 to 5 μM. These observations suggested that the dihydropyridines most likely compete for the binding of both [^{125}I]IAAP and [^{3}H]azidopine to the transporter. Similarly, FTC also inhibits photo-cross-linking of the transporter in R482-ABCG2 HEK cells with [^{125}I]IAAP in a concentration-dependent manner with an IC$_{50}$ of 5.0−5.5 μM (data not shown).

[**^{125}**I]IAAP Is Transported by ABCG2, and Nicardipine Inhibits the Transport of This Photoaffinity Analogue. [^{125}I]-IAAP and [^{3}H]azidopine have been used to characterize the drug binding sites of P-gp, and prazosin and several of its derivatives are known substrates of both ABCG2 and P-gp (*24*, *29*). We tested whether [^{125}I]IAAP is a transport substrate of ABCG2 using intact cell accumulation assays. MCF-7 (control), MCF-7 FLV1000, or MCF-7 AdVp3000 cells were incubated in subdued light with 1.5 nM [^{125}I]IAAP in the absence or presence of 10 μM FTC at 32 °C for 0−60 min. After being incubated, the cells were washed, and the radioactive analogues that had accumulated in the cells were assessed as described in Materials and Methods. While the wild-type ABCG2-expressing MCF-7 FLV1000 and mutant ABCG2-expressing MCF-7 AdVp3000 cells had a minimal level of [^{125}I]IAAP accumulation during the 60 min time course (Figure 3a), the control MCF-7 cells accumulated markedly higher levels. The presence of 10 μM FTC resulted in increased level of accumulation of the analogue in both MCF-7 FLV1000 and MCF-7 AdVp3000 cells at all time points examined. Nicardipine, which was more potent than nifedipine in inhibiting [^{125}I]IAAP photolabeling (Figure 1a), was evaluated for its ability to inhibit the transport of [^{125}I]-IAAP. As shown in Figure 3b, nicardipine (50 μM) inhibited the efflux of [^{125}I]IAAP in MCF-7 FLV1000 (70−75%) and MCF-7 AdVp3000 (80−85%) cells compared to the inhibition obtained with 10 μM FTC (100%) in these cells.

[**^{3}**H]Azidopine Is Transported by ABCG2, and Nicardipine Inhibits Its Transport. We found that [^{3}H]azidopine (dihydropyridine analogue) was able to photolabel ABCG2 (Figure 1c,d) and that nicardipine inhibited this labeling. Therefore, we tested [^{3}H]azidopine to see if it was a substrate of ABCG2. MCF-7 (control), MCF-7 FLV1000, or MCF-7 AdVp3000 cells were incubated in subdued light with 25 nM [^{3}H]azidopine in the absence or presence of 10 μM FTC at 32 °C for 0−60 min. The accumulation of [^{3}H]azidopine was assessed as described above. MCF-7 FLV1000 and MCF-7 AdVp3000 cells had reduced levels of accumulation compared to the MCF-7 control cells (Figure 4a) at all time points. This ABCG2-mediated efflux of [^{3}H]azidopine was inhibited by 10 μM FTC. The MCF-7 FLV1000 cells expressing R482-ABCG2 were less efficient at effluxing [^{3}H]-azidopine than MCF-7 AdVp3000 cells expressing T482-ABCG2 (Figure 4a), perhaps due to the differences in the substrate specificity of the wild-type and mutant transporter. Nicardipine (50 μM) inhibited the ABCG2-mediated efflux of [^{3}H]azidopine in both the wild-type and mutant ABCG2-expressing MCF-7 FLV1000 and MCF-7 AdVp3000 cells,

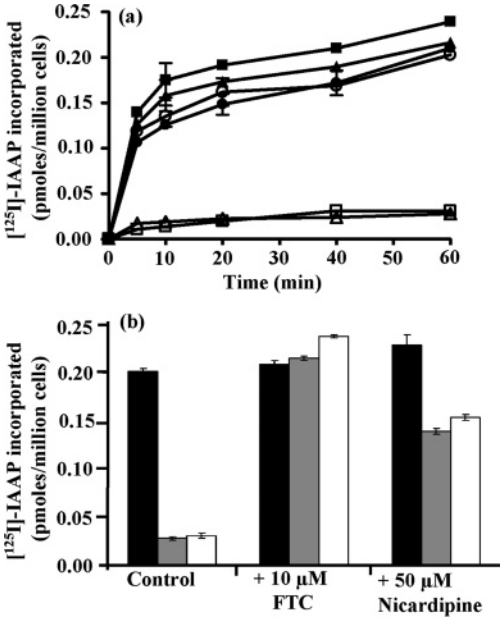

FIGURE 3: [^{125}I]IAAP is a transport substrate of both wild-type and mutant ABCG2, and nicardipine inhibits this transport. (a) The control MCF-7 (○ and ●), MCF-7 FLV1000 (△ and ▲), and MCF-7 AdVp3000 (□ and ■) cells (0.25×10^6 cells/well) were incubated with 3−5 nM [^{125}I]IAAP in the absence (empty symbols) or presence (filled symbols) of 10 μM FTC at 32 °C for varying times (0−60 min) in RPMI medium supplemented with 5% FBS. After being incubated, cells were washed with 1 mL of ice-cold PBS and lysed by trypsinization in 0.3 mL of a trypsin-EDTA solution. The amount of radioactive drug accumulated inside the cells was measured by liquid scintillation counting. The graph shows the amount of [^{125}I]IAAP that accumulated (picomoles per 1 million cells) as a function of time in the presence or absence of 10 μM FTC. The mean value from three independent experiments which were performed in duplicate is shown here, and error bars indicate the standard deviation. (b) The control MCF-7 (black), MCF-7 FLV1000 (gray), and MCF-7 AdVp3000 (white) cells were incubated with 3−5 nM [^{125}I]IAAP in the absence (control) or presence of either 10 μM FTC or 50 μM nicardipine at 32 °C for 60 min in RPMI medium supplemented with 5% FBS. After being incubated, cells were washed, lysed, and processed as described above. The histogram shows the amount of [^{125}I]IAAP that accumulated (picomoles per 1 million cells) in the cells in the absence (control) or presence of either 10 μM FTC or 50 μM nicardipine. The mean values with error bars (±standard deviation) from three independent experiments performed in duplicate are shown.

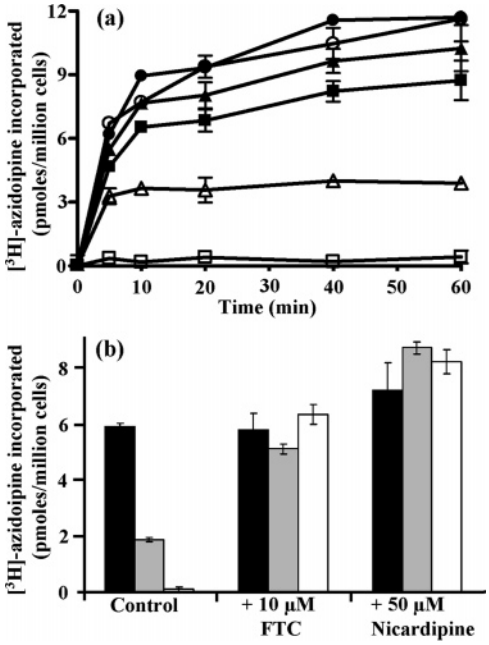

FIGURE 4: [^{3}H]Azidopine is a transport substrate of both wild-type and mutant ABCG2, and nicardipine inhibits this transport. (a) The control MCF-7 (○ and ●), MCF-7 FLV1000 (△ and ▲), and MCF-7 AdVp3000 (■ and □) cells (0.25×10^6 cells/well) were incubated with 25 nM [^{3}H]azidopine in the absence (empty symbols) or presence (filled symbols) of 10 μM FTC at 32 °C for varying times (0−60 min) in RPMI medium supplemented with 5% FBS. After being incubated, cells were washed, lysed, and processed as described in the legend of Figure 3a. The graph shows the amount of [^{3}H]azidopine (picomoles per 1 million cells) as a function of time in the presence or absence of 10 μM FTC. The mean value from three independent experiments performed in duplicate is shown here, and error bars indicate the standard deviation. (b) Control MCF-7 (black), MCF-7 FLV1000 (gray), and MCF-7 AdVp3000 (white) cells were incubated with 25 nM [^{3}H]azidopine in the absence (control) or presence of 10 μM FTC or 50 μM nicardipine at 32 °C for 60 min in RPMI medium supplemented with 5% FBS. After being incubated, cells were washed, lysed, and processed as described in the legend of Figure 3a. The histogram shows the amount of [^{3}H]azidopine that accumulated (picomoles per 1 million cells) in the cells in the absence (control) or presence of 10 μM FTC or 50 μM nicardipine. The mean values with error bars (±standard deviation) from three independent experiments performed in duplicate are shown.

and this inhibition of efflux by nicardipine was comparable to the inhibition obtained with 10 μM FTC (Figure 4b). It should be noted that the inhibition of [^{3}H]azidopine efflux by nicardipine (Figure 4b) was more potent than the inhibition of [^{125}I]IAAP efflux (Figure 3b). This may be due to the differences in the chemical structure of azidopine and IAAP. Nicardipine and azidopine are both dihydropyridines, and nicardipine might inhibit the efflux of azidopine more efficiently than IAAP because of the similarity in chemical structure. These results for the first time demonstrate that [^{3}H]azidopine is a substrate for both wild-type and mutant ABCG2 and that nicardipine inhibits the efflux of this photoaffinity analogue from ABCG2-expressing cells.

Dihydropyridines Inhibit the Transport of Mitoxantrone and Pheophorbide-a in Wild-Type (R482) and Mutant (G482 and T482) ABCG2-Expressing Cells. The photolabeling and accumulation assays described above demonstrated that 1,4-dihydropyridines could effectively inhibit the photolabeling of ABCG2 and the efflux of both [^{125}I]IAAP and [^{3}H]-azidopine from ABCG2-expressing cells. Therefore, we tested the effect of these dihydropyridines on the accumulation of the known ABCG2 substrates mitoxantrone and pheophorbide-a (*8*, *28*). The ABCG2-transfected HEK and drug-selected ABCG2-overexpressing MCF-7 cells were used independently to rule out the possibility of changes in the activity of the protein when ABCG2 was overexpressed under the CMV promoter in HEK cells or under the native promoter in MCF-7 cells. Cells were incubated with 5 μM mitoxantrone or pheophorbide-a in combination with varying concentrations of nicardipine, nifedipine, or 10 μM FTC, a specific inhibitor of ABCG2, and then incubated at 37 °C in the dark for 45 min. The accumulation of these substrates was assessed by flow cytometry, as described in Materials and Methods. Representative histograms in the presence and absence of 40 μM nicardipine are shown in Figure 5. The presence of 40 μM nicardipine and nifedipine increased the accumulation of mitoxantrone (Figure 5a−f) and pheophor-

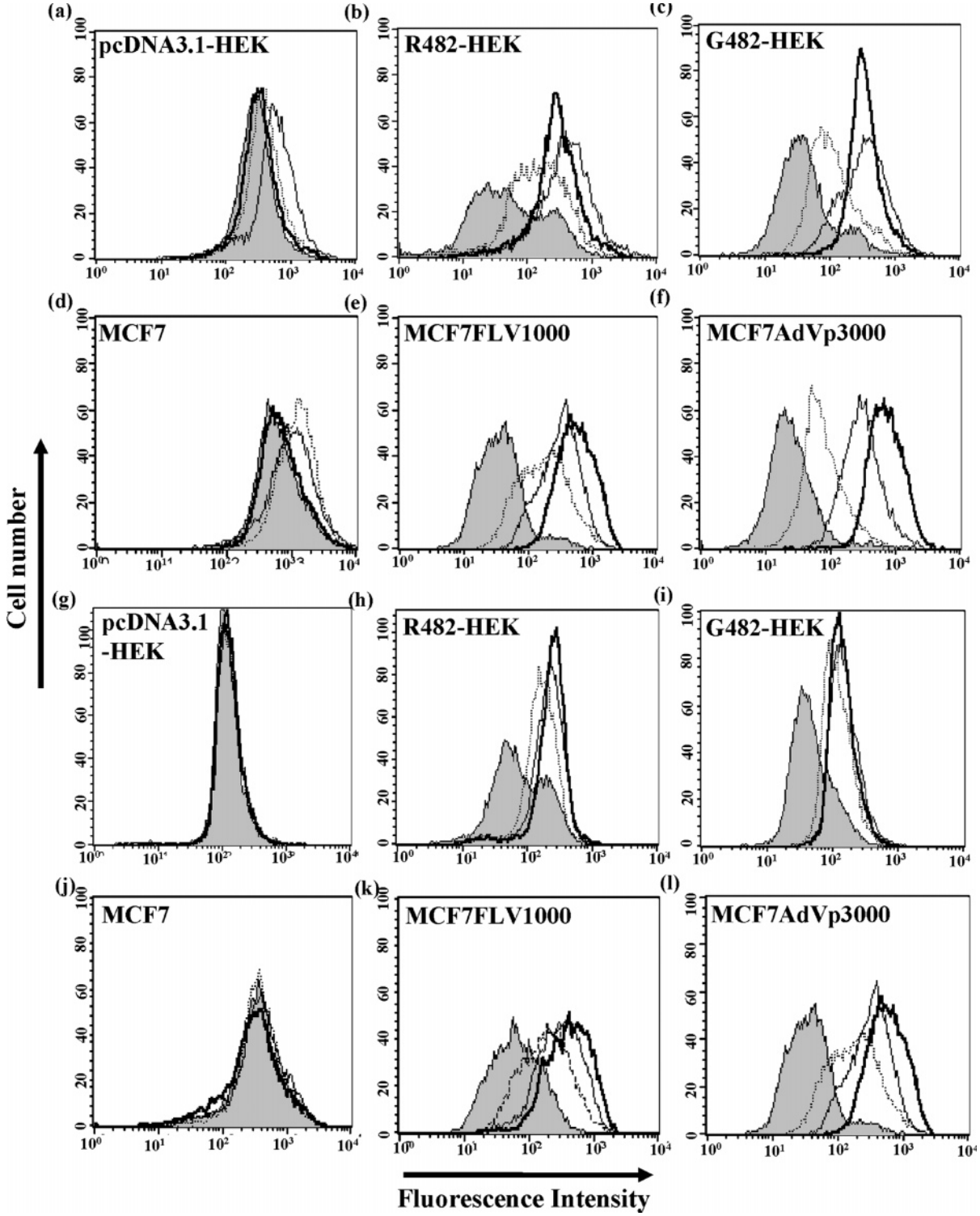

FIGURE 5: Dihydropyridines inhibit the ABCG2-mediated efflux of mitoxantrone and pheophorbide-a. pcDNA3.1-HEK (a and g), R482-HEK (b and h), G482-HEK (c and i), MCF-7 (d and j), MCF-7 FLV1000 (e and k), and MCF-7 AdVp3000 (f and l) cells were incubated with 5 μM mitoxantrone (a−f) or pheophorbide-a (g−l) for 45 min at 37 °C, in the presence of 40 μM nicardipine (thin lines), nifedipine (broken lines), or 10 μM FTC (thick lines). The cells were then pelleted and resuspended in PBS with 0.1% BSA and analyzed. The histogram derived from CellQuest which depicts the fluorescence intensity of the cells on the *X*-axis and the cell number on the *Y*-axis is shown here. The shaded histogram represents the control DMSO-treated cells.

bide-a (Figure 5g−l) in R482-HEK, G482-HEK, MCF-7 FLV1000, and MCF-7 AdVp3000 cells. We also used varying concentrations (0−75 μM) of nicardipine and nifedipine and observed that the inhibition of mitoxantrone and pheophorbide-a transport by dihydropyridines in both wild-type (Figure 6a,c) and mutant (Figure 6b,d) ABCG2-expressing HEK and MCF-7 cells was concentration-dependent. Similar results were also obtained with the inhibition of pheophorbide-a transport by these compounds (Figure 6e−h). It should be noted that the accumulation of mitoxantrone (Figure 6a−d) and pheophorbide-a (Figure 6e−h) was maximum in the cells incubated with nicardipine in

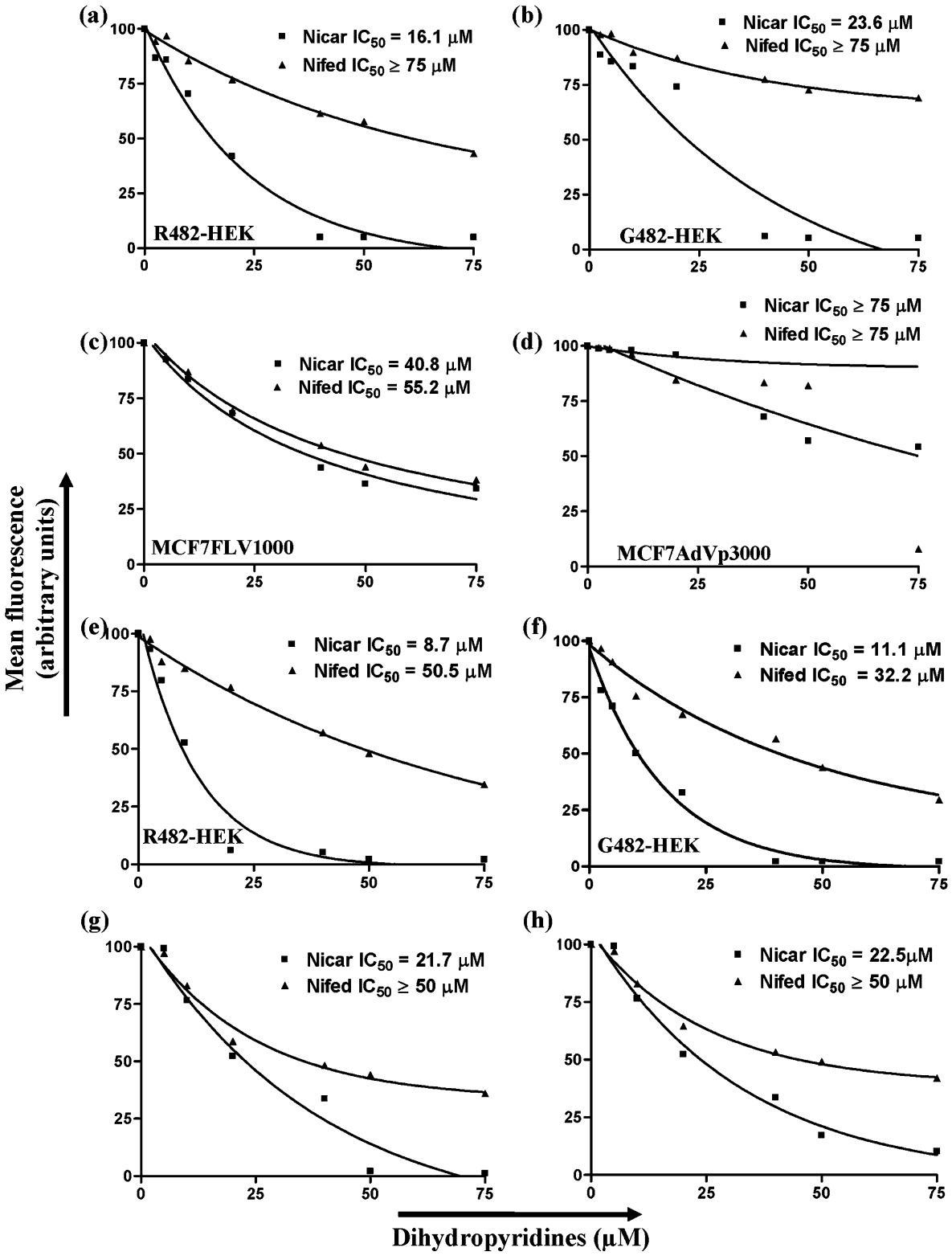

FIGURE 6: Inhibition of mitoxantrone and pheophorbide-a transport by dihydropyridines is concentration-dependent. R482-HEK (a and e), G482-HEK (b and f), MCF-7 FLV1000 (c and g), and MCF-7 AdVp3000 (d and h) cells were incubated with 5 μM mitoxantrone (a−d) or pheophorbide-a (e−h) for 45 min at 37 °C in the presence of varying concentrations (0−75 μM) of nicardipine (■) or nifedipine (▲). The cells were then pelleted, resuspended in PBS with 0.1% BSA, and analyzed as described in Materials and Methods, and the mean fluorescent intensities were calculated with CellQuest. The difference in the mean fluorescence intensity in the presence of 10 μM FTC and in the absence of dihydropyridine was taken to be 100% (control) and assigned an arbitrary value of 100. The differences in the mean fluorescence intensity values in the presence of 10 μM FTC and the indicated concentration of dihydropyridines were calculated as a percent of the control. The *Y*-axis in the graphs represents the difference between the mean fluorescence intensity values in the presence of 10 μM FTC and the given concentration of dihydropyridine, which is plotted as a function of the concentration of the indicated dihydropyridine (*X*-axis). The mean values from three independent experiments performed in triplicate are plotted, and the data were fitted using Graphpad Prism version 2.0. There was <10% variation in each data set. The IC_{50} values given in each panel represent the concentration which inhibited the efflux to 50% of the control values. Nicar represents nicardipine and Nifed nifedipine.

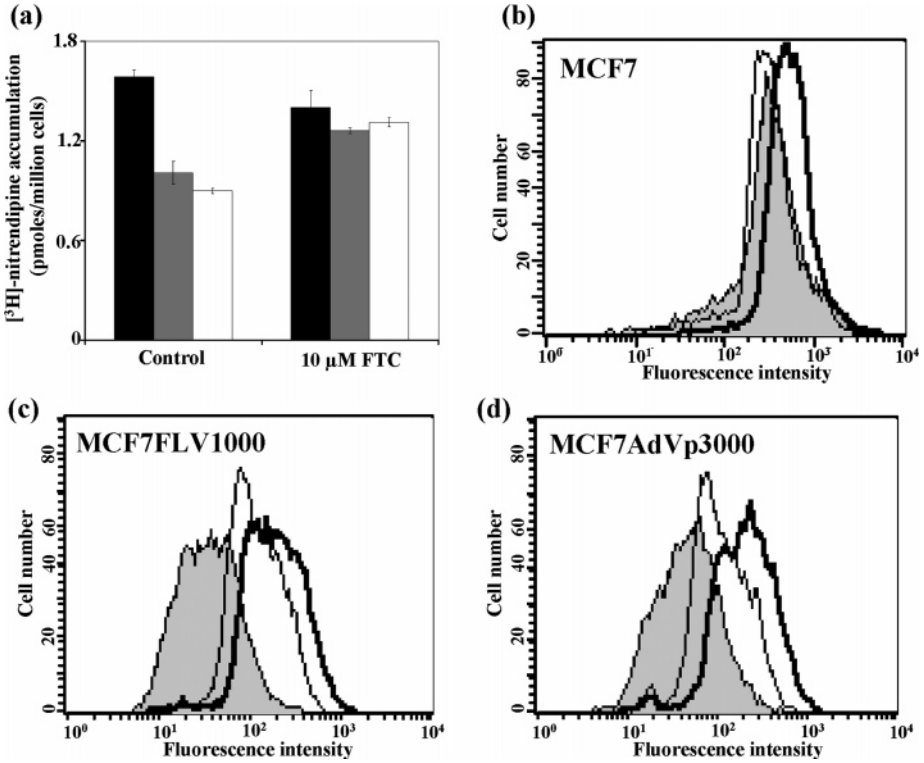

FIGURE 7: [^{3}H]Nitrendipine and bodipy-Fl-dihydropyridine are transported by the wild-type ABCG2-expressing MCF-7 FLV1000 and mutant ABCG2-expressing MCF-7 AdVp3000 cells. (a) The control MCF-7 (black), MCF-7 FLV1000 (gray), and MCF-7 AdVp3000 (white) cells were incubated with 25 nM [^{3}H]nitrendipine in the absence (control) or presence of 10 μM FTC at 32 °C for 60 min in RPMI medium supplemented with 5% FBS. After being incubated, cells were washed, lysed, and processed as described in the legend of Figure 3a. The histogram shows the amount of [^{3}H]nitrendipine that accumulated (picomoles per 1 million cells) in the cells in the absence (control) or presence of 10 μM FTC. (b−d) MCF-7, MCF-7 FLV1000, and MCF-7 AdVp3000 cells were incubated with 0.5 μM bodipy-Fl-dihydropyridine in the absence or presence of 10 μM FTC or 25 μM nicardipine at 37 °C for 45 min in the dark. After 45 min, the cells were pelleted, washed, and analyzed as described in Materials and Methods. The histogram, derived from CellQuest which depicts the fluorescence intensity of the cells on the *X*-axis and the cell number on the *Y*-axis, depicts cells treated with DMSO control (gray filled) or 10 μM FTC (thick lines) or 25 μM nicardipine (thin lines) from one representative experiment. Similar results were obtained in two additional experiments.

both wild-type and mutant ABCG2-expressing HEK and MCF-7 cells (see the IC_{50} values in individual panels in Figure 6). It should be noted that the MCF-7 FLV1000 cell line does express high levels of R482-ABCG2 compared to the level of expression in transfected R482-HEK-293 cells (data not shown). For this reason, it is possible that the concentration of nicardipine, which produces a distinct effect in HEK-293 cells, may not be enough to inhibit the transport mediated by ABCG2 in MCF-7 FLV1000 cells. On the other hand, nicardipine was better in inhibiting the efflux of pheophorbide-a in this cell line than nifedipine (Figure 6g). The observed possible differences could also be caused by the affinity of the substrates, mitoxantrone and pheophorbide-a, for wild-type R482-ABCG2.

Dihydropyridines Are Transport Substrates of ABCG2. The accumulation assays described above ([^{125}I]IAAP, [^{3}H]-azidopine, mitoxantrone, and pheophorbide-a) demonstrated that dihydropyridines, nicardipine and nifedipine, can be used to inhibit ABCG2-mediated efflux. To further confirm if dihydropyridines themselves are substrates of ABCG2, we determined the ability of wild-type and mutant ABCG2-expressing MCF-7 FLV1000 and MCF-7 AdVp3000 cells to efflux [^{3}H]nitrendipine, another 1,4-dihydropyridine antihypertensive agent. The MCF-7 FLV1000 and MCF-7 AdVp3000 cells were incubated with 25 nM [^{3}H]nitrendipine in the presence or absence of 10 μM FTC for 60 min, and the accumulation of radiolabeled nitrendipine in control and ABCG2-expressing cells was assessed as described in Materials and Methods. It was observed that, while the control MCF-7 cells accumulated 1.58 pmol/1 million cells of [^{3}H]nitrendipine, the ABCG2-expressing MCF-7 FLV1000 and MCF-7 AdVp3000 cells accumulated 0.90 and 0.81 pmol/1 million cells of [^{3}H]nitrendipine (Figure 7a), respectively. The presence of 10 μM FTC increased the level of accumulation of [^{3}H]nitrendipine in both the wild-type and mutant ABCG2-expressing MCF-7 FLV1000 and MCF-7 AdVp3000 cells. We also used a fluorescent analogue of dihydropyridine, bodipy-Fl-dihydropyridine, in the FACS assay to determine if it was also a substrate of ABCG2. The MCF-7 FLV1000 and MCF-7 AdVp3000 cells effluxed bodipy-Fl-dihydropyridine (Figure 7c,d), and the presence of either 10 μM FTC or 25 μM nicardipine inhibited this efflux; the control MCF-7 cells were not able to efflux this compound (Figure 7b). Taken together with the [^{3}H]-azidopine accumulation experiments (Figure 6), this demonstrates that dihydropyridines are indeed transported by ABCG2.

Inhibition of ABCG2-Mediated Drug Resistance by Dihydropyridines. The results shown in Figures 3−5 and 7 suggested that nicardipine and nifedipine inhibit the ABCG2-mediated efflux of substrates from the cells. Therefore, it was expected that the presence of nicardipine and nifedipine

Table 1: Reversal of Resistance in ABCG2-Expressing HEK-293 Cells to Mitoxantrone with 10 μM Dihydropyridines

cell line	cytotoxicity of mitoxantrone, IC_{50} (nM)[a] (relative resistance)[b]		
	control (DMSO)	with 10 μM nicardipine	with 10 μM nifedipine
pcDNA3.1-HEK-293	9.4 ± 2.7 (1)	12.4 ± 4.3 (1)	16.2 ± 3.2 (1)
R482-HEK-293 (wild-type)	186.0 ± 9.1 (19.8)	62.1 ± 5.7 (5.0)	71.3 ± 3.2 (4.4)
G482-HEK-293	483.4 ± 23.7 (51.4)	164.9 ± 6.3 (13.3)	178.9 ± 10.4 (11.1)

[a] The values represent the means ± the standard deviation of three independent experiments performed in triplicate. [b] Relative resistance values (in parentheses) were obtained by dividing the IC_{50} value of the R482-HEK-293 or G482-HEK-293 cells by the IC_{50} value of the empty vector pcDNA-HEK-293 transfected cell line.

would sensitize ABCG2-expressing cells to drug substrates of this transporter. The cytotoxicity of mitoxantrone to ABCG2-expressing HEK cells was determined in the presence of nontoxic concentrations (10 μM) of nicardipine and nifedipine. As shown in Table 1, the IC_{50} values of mitoxantrone for pcDNA3.1-HEK, R482-HEK, and G482-HEK cells were 9.4, 186.0, and 483.4 nM, respectively. The presence of 10 μM nicardipine or nifedipine did not have any significant effect on the IC_{50} value of mitoxantrone in the control pcDNA3.1-HEK cells, but it did result in an approximately 3−5-fold decrease in the IC_{50} value of mitoxantrone in R482- and G482-HEK ABGC2-expressing cells (Table 1). These observations suggested that nontoxic concentrations of the dihydropyridines inhibit the drug resistance mediated by ABCG2, thereby making ABCG2-expressing cells more sensitive to mitoxantrone.

Dihydropyridines Stimulate ATP Hydrolysis by ABCG2. It is known that ABC drug transporters utilize the energy of ATP hydrolysis to transport drugs outside cells. The presence of the drug stimulates ATP hydrolysis by the transporter (*30*, *31*). Since dihydropyridines are substrates of ABCG2 and interact with the substrate binding sites of the transporter, we examined the effect of dihydropyridines on the ATPase activity in the crude membranes isolated from R482-ABCG2-expressing HEK cells. As shown in Figure 8a, the presence of varying concentrations of both nicardipine and nifedipine stimulated ATP hydrolysis by ABCG2 in a concentration-dependent manner. The maximal fold stimulation obtained with nifedipine was ~3.0−3.5-fold, while nicardipine stimulated the ATPase activity to ~1.8−2.0-fold of the basal activity. The level of stimulation of the ATPase activity by nifedipine was comparable to or greater than the level of stimulation by prazosin, which is a known substrate for ABCG2, at all concentrations. We also determined the effect of FTC on nifedipine-stimulated ATPase activity. We used nifedipine (5 μM) to stimulate the ATP hydrolysis mediated by R482-ABCG2 and determined the effect of varying concentrations of FTC (0−10 μM) on this activity. As shown in Figure 8b, the presence of FTC inhibited nifedipine-stimulated ATP hydrolysis by R482-ABCG2 in a concentration-dependent manner with an IC_{50} value of 0.51 μM.

To test whether the dihydropyridines interact at the nucleotide-binding site of ABCG2, we determined the effect of dihydropyridines on the photolabeling of ABCG2 with [α-^{32}P]-8-azido-ATP, a photoaffinity analogue of ATP. It was observed that while [α-^{32}P]-8-azido-ATP was able to photolabel ABCG2, the presence of 25 μM nicardipine and nifedipine did not inhibit the incorporation of [α-^{32}P]-8-azido-ATP into ABCG2 (data not shown). These observations suggested that the stimulation of ATPase activity by dihydropyridines was due to their interaction at the drug substrate site(s) of the transporter.

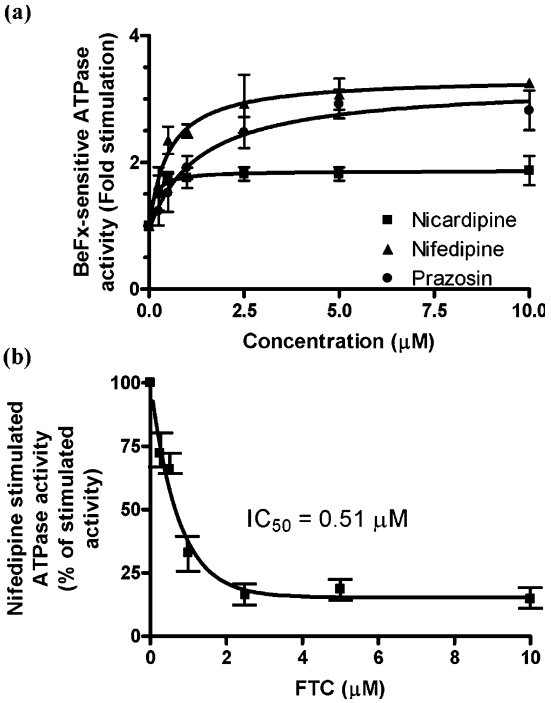

FIGURE 8: Dihydropyridines stimulate BeFx-sensitive ATPase activity, and FTC inhibits the nifedipine-stimulated ATPase activity of ABCG2. (a) Crude membranes from R482-HEK cells (100 μg of protein/mL) were incubated at 37 °C with varying concentrations of nicardipine (■), nifedipine (▲), or prazosin (●) in the presence and absence of BeFx (0.2 mM beryllium sulfate and 2.5 mM sodium fluoride) in ATPase assay buffer for 5 min. The reaction was started by the addition of 5 mM ATP, and after 20 min at 37 °C, the assay was stopped by the addition of 0.1 mL of a 5% SDS solution. The amount of inorganic phosphate released and the BeFx-sensitive ATPase activity of ABCG2 were determined as described in Materials and Methods. The fold stimulation of ATPase activity (mean values ± the standard deviation) from three independent experiments is plotted as a function of the increasing concentration of the tested compounds. The basal ATPase activity in the absence of the drug was in the range of 15−20 nmol of P_i min^{-1} (mg of protein)$^{-1}$. (b) Crude membranes from R482-HEK cells (100 μg of protein/mL) were incubated at 37 °C with 5 μM nifedipine and the indicated concentration of FTC (■) in the presence and absence of BeFx in ATPase assay buffer for 5 min. The reaction was started by the addition of 5 mM ATP. The assay was stopped after 20 min and processed as described above. The graph represents the percent inhibition of the nifedipine-stimulated ATPase activity (*Y*-axis) (mean values ± the standard deviation from three independent experiments) as a function of varying concentrations of FTC (*X*-axis).

DISCUSSION

Development of multidrug resistance (MDR) is a problem in cancer chemotherapy that limits the effectiveness of

anticancer drugs (*30*, *32*). ABCG2 is a half-transporter of the ABCG subfamily of ABC transporters whose overexpression has been shown to be linked with the development of the MDR phenotype in malignant cells (*6*, *33*−*35*). One of the possible mechanisms by which the development of MDR can be circumvented during chemotherapy is blocking of the functions of this ABC transporter, and there is a need to develop suitable inhibitors for this transporter. In an attempt to develop assays for screening inhibitors and to characterize their interaction with ABCG2, we used the two photoaffinity analogues, [^{125}I]IAAP and [^{3}H]azidopine, as investigative tools.

We showed here that both [^{125}I]IAAP and [^{3}H]azidopine can be used to label wild-type (R482) and mutant (T482) ABCG2 (Figure 1). It has been shown that [^{125}I]IAAP and a photoaffinity analogue of rhodamine 123, iodoarylazidorhodamine 123, can photolabel ABCG2 (*24*, *36*), but this is the first report showing that [^{3}H]azidopine can also be used to photolabel ABCG2. In addition, we used these two analogues in an intact cell accumulation assay and demonstrated that both of them are transported by ABCG2 (Figures 3 and 4). Though there was a difference in the ability of the wild-type and mutant ABCG2 to transport the [^{3}H]azidopine (Figure 4a), both variants transported this analogue. We showed that these two assays could further be used to study drug interactions with this transporter and in our screening assays observed that 1,4-dihydropyridines inhibited the labeling of these agents. The level of inhibition was comparable to that obtained with FTC, a well-known inhibitor of ABCG2 (Figure 1). We also used the labeling and accumulation assays with other known ABCG2 substrates and inhibitors such as mitoxantrone, pheophorbide-a, and Ko143 to validate the assays and observed that all of them inhibited the binding as well as efflux of these analogues (data not shown). Both IAAP and azidopine label ABCG2 at very low (nanomolar) concentrations, and higher concentrations of anticancer agents or dihydropyridines are required to inhibit this labeling, suggesting that these photolabels exhibit a higher affinity for ABCG2. However, the detailed characterization of the affinity of IAAP and azidopine for ABCG2 needs to be carried out.

Zhou et al. (*37*) recently reported that dihydropyridines and their structural derivatives could inhibit the drug resistance mediated by ABCG2 and demonstrated in in vivo studies that one of the dihydropyridine derivatives, DHP-014, produced a 2-fold increase in the level of systemic exposure of topotecan and significantly enhanced the peak concentration of oral topotecan in rats. These authors speculated that the observed increase in the systemic exposure levels of topotecan was due to the inhibition of ABCG2 present on the apical surface of intestinal epithelium, thereby increasing the amount of topotecan entering the circulation. Very recently, Zhang et al. (*38*) also reported that these dihydropyridines are inhibitors of ABCG2.

Both these studies did not elucidate the mechanism of interaction of dihydropyridines with ABCG2. Here we show a direct interaction of dihydropyridines with wild-type and mutant ABCG2 using the photoaffinity labeling experiments which demonstrate the interaction of these compounds at the drug substrate binding sites. It should be noted that azidopine itself is a dihydropyridine and its ability to photolabel ABCG2 indicated an interaction of dihydropyridines with the transporter. Both nicardipine and nifedipine competed for the photo-cross-linking of [^{125}I]IAAP and [^{3}H]azidopine to wild-type as well as mutant ABCG2, but nicardipine was most efficient in inhibiting the labeling with these two analogues. We also carried out accumulation assays using two other dihydropyridines, [^{3}H]nitrendipine and bodipy-Fl-dihydropyridine (Figure 7), and observed that both of them were transported by wild-type and mutant ABCG2. These results are different from the observations of Zhang et al. (*38*), who showed that [^{3}H]nitrendipine was not transported by R482-ABCG2-expressing cells. The possible differences in the results could be caused by the low chemical concentration of [^{3}H]nitrendipine that was used (10 nM) and the relatively lower level of expression of ABCG2 in HEK cells used for accumulation assays by Zhang et al. (*35*). On the other hand, we used 25 nM [^{3}H]nitrendipine and MCF-7 FLV1000 and MCF-7 AdVp3000 cells which do express very high levels of ABCG2 compared to ABCG2-expressing HEK cells (our unpublished data). Moreover, we used three different dihydropyridines, azidopine (Figure 4), [^{3}H]nitrendipine, and bodipy-Fl-dihydropyridine (Figure 7), in different assays, which consistently confirmed that these are substrates of ABCG2.

Many transport substrates stimulate ATP hydrolysis by ABC transporters, and our experiments suggested that dihydropyridines are transported by ABCG2. To confirm this, we also determined the effect of dihydropyridines on the ATPase activity of ABCG2. It was observed that both nicardipine and nifedipine stimulated ATP hydrolysis by the transporter (Figure 8), and this maximal stimulation by nifedipine was equal to or greater than that obtained with prazosin, a known substrate of ABCG2. We also determined the effect of FTC on the nifedipine-stimulated ATPase activity and found that it inhibited the stimulation of ATPase activity in a concentration-dependent manner, which is consistent with its inhibition of photolabeling and drug accumulation. On the basis of these results, we speculate that dihydropyridines might share the substrate-binding pocket with FTC, and further work is required to verify this. Taken together, results from the transport assays, the photoaffinity labeling, and the ATPase studies provide convincing evidence that dihydropyridines are transported by ABCG2. Additionally, we show that nontoxic concentrations (10 μM) of nicardipine and nifedipine render the ABCG2-expressing cells sensitive to mitoxantrone (Table 1).

The dihydropyridines we tested are clinically used as antihypertensive drugs, and the fact that these drugs are substrates of ABCG2 indicates that ABCG2 might be an important determinant for their potency and use for the treatment of hypertension. The fact that these dihydropyridines (antihypertensive agents) are substrates of human ABCG2 indicates the potential risk of neonatal exposure through excretion and concentration of these drugs in breast milk, similar to the risk posed by the transport of other drugs and antibiotics by ABGC2, as reported recently (*13*).

In conclusion, we have used photoaffinity labeling and efflux assays to study drug interactions with ABCG2. We demonstrate the use of these photoaffinity agents in characterizing the interaction of dihydropyridines with ABCG2 at biochemical levels and have shown that dihydropyridines are substrates of this transporter. The use of [^{125}I]IAAP and [^{3}H]azidpoine for photo-cross-linking and transport assays

provides valuable tools for screening potential substrates and inhibitors and for studying the drug-binding site(s) of this transporter.

ACKNOWLEDGMENT

We are thankful to Dr. Michael M. Gottesman for encouragement and Drs. Anna Calcagno, In-Wha Kim, and Zuben Sauna for discussions and comments on the manuscript. We also thank George Leiman for assistance in the preparation of the manuscript.

REFERENCES

1. Allikmets, R., Schriml, L. M., Hutchinson, A., Romano-Spica, V., and Dean, M. (1998) A human placenta-specific ATP-binding cassette gene (ABCP) on chromosome 4q22 that is involved in multidrug resistance, *Cancer Res. 58*, 5337−9.
2. Doyle, L. A., Yang, W., Abruzzo, L. V., Krogmann, T., Gao, Y., Rishi, A. K., and Ross, D. D. (1998) A multidrug resistance transporter from human MCF-7 breast cancer cells, *Proc. Natl. Acad. Sci. U.S.A. 95*, 15665−70.
3. Miyake, K., Mickley, L., Litman, T., Zhan, Z., Robey, R., Cristensen, B., Brangi, M., Greenberger, L., Dean, M., Fojo, T., and Bates, S. E. (1999) Molecular cloning of cDNAs which are highly overexpressed in mitoxantrone-resistant cells: Demonstration of homology to ABC transport genes, *Cancer Res. 59*, 8−13.
4. Bates, S. E., Medina-Perez, W. Y., Kohlhagen, G., Antony, S., Nadjem, T., Robey, R. W., and Pommier, Y. (2004) ABCG2 mediates differential resistance to SN-38 (7-ethyl-10-hydroxycamptothecin) and homocamptothecins, *J. Pharmacol. Exp. Ther. 310*, 836−42.
5. Yoshikawa, M., Ikegami, Y., Sano, K., Yoshida, H., Mitomo, H., Sawada, S., and Ishikawa, T. (2004) Transport of SN-38 by the wild type of human ABC transporter ABCG2 and its inhibition by quercetin, a natural flavonoid, *J. Exp. Ther. Oncol. 4*, 25−35.
6. Maliepaard, M., van Gastelen, M. A., de Jong, L. A., Pluim, D., van Waardenburg, R. C., Ruevekamp-Helmers, M. C., Floot, B. G., and Schellens, J. H. (1999) Overexpression of the BCRP/MXR/ABCP gene in a topotecan-selected ovarian tumor cell line, *Cancer Res. 59*, 4559−63.
7. Scheffer, G. L., Maliepaard, M., Pijnenborg, A. C., van Gastelen, M. A., de Jong, M. C., Schroeijers, A. B., van der Kolk, D. M., Allen, J. D., Ross, D. D., van der Valk, P., Dalton, W. S., Schellens, J. H., and Scheper, R. J. (2000) Breast cancer resistance protein is localized at the plasma membrane in mitoxantrone- and topotecan-resistant cell lines, *Cancer Res. 60*, 2589−93.
8. Robey, R. W., Honjo, Y., Morisaki, K., Nadjem, T. A., Runge, S., Risbood, M., Poruchynsky, M. S., and Bates, S. E. (2003) Mutations at amino-acid 482 in the ABCG2 gene affect substrate and antagonist specificity, *Br. J. Cancer 89*, 1971−8.
9. Ozvegy-Laczka, C., Koblos, G., Sarkadi, B., and Varadi, A. (2005) Single amino acid (482) variants of the ABCG2 multidrug transporter: Major differences in transport capacity and substrate recognition, *Biochim. Biophys. Acta 1668*, 53−63.
10. Honjo, Y., Hrycyna, C. A., Yan, Q. W., Medina-Perez, W. Y., Robey, R. W., van de Laar, A., Litman, T., Dean, M., and Bates, S. E. (2001) Acquired mutations in the MXR/BCRP/ABCP gene alter substrate specificity in MXR/BCRP/ABCP-overexpressing cells, *Cancer Res. 61*, 6635−9.
11. Chen, Z. S., Robey, R. W., Belinsky, M. G., Shchaveleva, I., Ren, X. Q., Sugimoto, Y., Ross, D. D., Bates, S. E., and Kruh, G. D. (2003) Transport of methotrexate, methotrexate polyglutamates, and 17β-estradiol 17-(β-D-glucuronide) by ABCG2: Effects of acquired mutations at R482 on methotrexate transport, *Cancer Res. 63*, 4048−54.
12. Miwa, M., Tsukahara, S., Ishikawa, E., Asada, S., Imai, Y., and Sugimoto, Y. (2003) Single amino acid substitutions in the transmembrane domains of breast cancer resistance protein (BCRP) alter cross resistance patterns in transfectants, *Int. J. Cancer 107*, 757−63.
13. Jonker, J. W., Merino, G., Musters, S., van Herwaarden, A. E., Bolscher, E., Wagenaar, E., Mesman, E., Dale, T. C., and Schinkel, A. H. (2005) The breast cancer resistance protein BCRP (ABCG2) concentrates drugs and carcinogenic xenotoxins into milk, *Nat. Med. 11*, 127−9.
14. van Herwaarden, A. E., Wagenaar, E., Karnekamp, B., Merino, G., Jonker, J. W., and Schinkel, A. H. (2006) Breast cancer resistance protein (Bcrp1/Abcg2) reduces systemic exposure of the dietary carcinogens aflatoxin B1, IQ and Trp-P-1 but also mediates their secretion into breast milk, *Carcinogenesis 27*, 123−30.
15. Houghton, P. J., Germain, G. S., Harwood, F. C., Schuetz, J. D., Stewart, C. F., Buchdunger, E., and Traxler, P. (2004) Imatinib mesylate is a potent inhibitor of the ABCG2 (BCRP) transporter and reverses resistance to topotecan and SN-38 in vitro, *Cancer Res. 64*, 2333−7.
16. Burger, H., van Tol, H., Brok, M., Wiemer, E. A., de Bruijn, E. A., Guetens, G., de Boeck, G., Sparreboom, A., Verweij, J., and Nooter, K. (2005) Chronic Imatinib Mesylate Exposure Leads to Reduced Intracellular Drug Accumulation by Induction of the ABCG2 (BCRP) and ABCB1 (MDR1) Drug Transport Pumps, *Cancer Biol. Ther. 4*, 747−52.
17. Robey, R. W., Medina-Perez, W. Y., Nishiyama, K., Lahusen, T., Miyake, K., Litman, T., Senderowicz, A. M., Ross, D. D., and Bates, S. E. (2001) Overexpression of the ATP-binding cassette half-transporter, ABCG2 (Mxr/BCrp/ABCP1), in flavopiridol-resistant human breast cancer cells, *Clin. Cancer Res. 7*, 145−52.
18. Chearwae, W., Anuchapreeda, S., Nandigama, K., Ambudkar, S. V., and Limtrakul, P. (2004) Biochemical mechanism of modulation of human P-glycoprotein (ABCB1) by curcumin I, II, and III purified from Turmeric powder, *Biochem. Pharmacol. 68*, 2043−52.
19. Ambudkar, S. V. (1998) Drug-stimulatable ATPase activity in crude membranes of human MDR1-transfected mammalian cells, *Methods Enzymol. 292*, 504−14.
20. Greenberger, L. M. (1998) Identification of drug interaction sites in P-glycoprotein, *Methods Enzymol. 292*, 307−17.
21. Shukla, S., Saini, P., Smriti, Jha, S., Ambudkar, S. V., and Prasad, R. (2003) Functional characterization of *Candida albicans* ABC transporter Cdr1p, *Eukaryotic Cell 2*, 1361−75.
22. Hanson, L., May, L., Tuma, P., Keeven, J., Mehl, P., Ferenz, M., Ambudkar, S. V., and Golin, J. (2005) The role of hydrogen bond acceptor groups in the interaction of substrates with Pdr5p, a major yeast drug transporter, *Biochemistry 44*, 9703−13.
23. Reuter, G., Janvilisri, T., Venter, H., Shahi, S., Balakrishnan, L., and van Veen, H. W. (2003) The ATP binding cassette multidrug transporter LmrA and lipid transporter MsbA have overlapping substrate specificities, *J. Biol. Chem. 278*, 35193−8.
24. Ejendal, K. F., and Hrycyna, C. A. (2005) Differential sensitivities of the human ATP-binding cassette transporters ABCG2 and P-glycoprotein to cyclosporine A, *Mol. Pharmacol. 67*, 902−11.
25. Rabindran, S. K., He, H., Singh, M., Brown, E., Collins, K. I., Annable, T., and Greenberger, L. M. (1998) Reversal of a novel multidrug resistance mechanism in human colon carcinoma cells by fumitremorgin C, *Cancer Res. 58*, 5850−8.
26. Rabindran, S. K., Ross, D. D., Doyle, L. A., Yang, W., and Greenberger, L. M. (2000) Fumitremorgin C reverses multidrug resistance in cells transfected with the breast cancer resistance protein, *Cancer Res. 60*, 47−50.
27. Garimella, T. S., Ross, D. D., Eiseman, J. L., Mondick, J. T., Joseph, E., Nakanishi, T., Bates, S. E., and Bauer, K. S. (2005) Plasma pharmacokinetics and tissue distribution of the breast cancer resistance protein (BCRP/ABCG2) inhibitor fumitremorgin C in SCID mice bearing T8 tumors, *Cancer Chemother. Pharmacol. 55*, 101−9.
28. Robey, R. W., Steadman, K., Polgar, O., Morisaki, K., Blayney, M., Mistry, P., and Bates, S. E. (2004) Pheophorbide a is a specific probe for ABCG2 function and inhibition, *Cancer Res. 64*, 1242−6.
29. Greenberger, L. M., Yang, C. P., Gindin, E., and Horwitz, S. B. (1990) Photoaffinity probes for the α1-adrenergic receptor and the calcium channel bind to a common domain in P-glycoprotein, *J. Biol. Chem. 265*, 4394−401.
30. Ambudkar, S. V., Dey, S., Hrycyna, C. A., Ramachandra, M., Pastan, I., and Gottesman, M. M. (1999) Biochemical, cellular, and pharmacological aspects of the multidrug transporter, *Annu. Rev. Pharmacol. Toxicol. 39*, 361−98.
31. Sarkadi, B., Ozvegy-Laczka, C., Nemet, K., and Varadi, A. (2004) ABCG2: A transporter for all seasons, *FEBS Lett. 567*, 116−20.
32. Gottesman, M. M., Fojo, T., and Bates, S. E. (2002) Multidrug resistance in cancer: Role of ATP-dependent transporters, *Nat. Rev. Cancer 2*, 48−58.

33. Ross, D. D., Yang, W., Abruzzo, L. V., Dalton, W. S., Schneider, E., Lage, H., Dietel, M., Greenberger, L., Cole, S. P., and Doyle, L. A. (1999) Atypical multidrug resistance: Breast cancer resistance protein messenger RNA expression in mitoxantrone-selected cell lines, *J. Natl. Cancer Inst. 91*, 429−33.
34. Yang, C. H., Schneider, E., Kuo, M. L., Volk, E. L., Rocchi, E., and Chen, Y. C. (2000) BCRP/MXR/ABCP expression in topotecan-resistant human breast carcinoma cells, *Biochem. Pharmacol. 60*, 831−7.
35. Haimeur, A., Conseil, G., Deeley, R. G., and Cole, S. P. (2004) The MRP-related and BCRP/ABCG2 multidrug resistance proteins: Biology, substrate specificity and regulation, *Curr. Drug Metab. 5*, 21−53.
36. Alqawi, O., Bates, S., and Georges, E. (2004) Arginine482 to threonine mutation in the breast cancer resistance protein ABCG2 inhibits rhodamine 123 transport while increasing binding, *Biochem. J. 382*, 711−6.
37. Zhou, X. F., Yang, X., Wang, Q., Coburn, R. A., and Morris, M. E. (2005) Effects of dihydropyridines and pyridines on multidrug resistance mediated by breast cancer resistance protein: In vitro and in vivo studies, *Drug Metab. Dispos. 33*, 1220−8.
38. Zhang, Y., Gupta, A., Wang, H., Zhou, L., Vethanayagam, R. R., Unadkat, J. D., and Mao, Q. (2005) BCRP transports dipyridamole and is inhibited by calcium channel blockers, *Pharm. Res. 22*, 2023−34.

BI060552F